として，安定化剤などを添加した試薬は，規定の試薬を用いたときと同等の結果を与えることを確認したうえで，使用可能であることを明記した．

旋光度測定法

測定温度が日局の標準温度である20℃に限定されていたため，USPやEPの標準温度25℃でも測定できるように，第一追補で，「……その測定は，通例，温度は20℃又は25℃，層長は……」と下線部を追記した．

窒素測定法

窒素測定法では，製薬業界からの要望で，自動化装置および市販の分解促進剤を使用可能な記載に改正した．自動化装置は，灰化部分と上流適定部分に分かれている装置が多いため，それぞれ単体でも導入できるようにした．また，自動適定装置では，指示薬などの差や，電位差適定法も包含されるような記載としている．自動化装置に関しては，装置の記載の後に，「ただし，有機物の分解，生成したアンモニアの蒸留及びその定量における適定終点検出法(電位差適定法，比色定量法など)など，自動化された装置を用いることができる」が追記された．また，自動化された装置を用いるにあたって，装置の適合性を確認することとした．標準試薬であるアミド硫酸を用いて，装置の指示通りの操作をするときに，窒素として99.0～101.0%が回収できる場合に装置として適合していると判断される．分解促進剤では，規定されたものと同等以上の結果を与えることを実試料を用いて検証してから，その種類と量を変更することができるとした．

重金属測定法

第3法の記載は，「医薬品各条に規定する量の試料を石英または磁性のるつぼに量り，初めは注意して弱く加熱し，強熱して灰化する」となっており，灰化温度の記載がなかったため，第二追補において，後半を，「加熱した後，500～600℃で強熱し，灰化する」と改正し，試験操作を明確化した．

残留溶媒試験法

日局における残留溶媒の取り扱い方針の変遷に伴い，日局16において若干の記載の修正を行った．日局15の第二追補では，残留溶媒は製造方法に依存するために，医薬品各条に一律に規定することは困難であるとして，医薬品各条に「別に規定する」と記載することとされた．その後，「別に規定する」こととなったことで，承認審査の場では，日局品であってもすべての残留溶媒試験法を個別に審査する必要が生じ，対応が困難であるという意見が出された．その後，個別の審査および医薬品各条での記載をしない方向で，「医薬品の残留溶媒ガイドライン」に基づいた総括的な考え方を通則に記載することで，すべての医薬品へ適応可能となり，GMP上の規制へと移行することとされた．しかし，製薬業界側から猶予期間が必要であるとの意見が出されたため，再度，日局16においては医薬品各条に「別に規定する」と記載し，通則への記載は日局17での対応を目指すことになった．

日局16における改正点は，上記の方針に従って，医薬品各条に有機溶媒の限度値を示すこと及び許容値を超えてはならないという記載を削除した．また，「医薬品の残留溶媒ガイドライン」に従って，ヒトに対して低毒性と考えられる溶媒のみが残留する場合には，乾

燥減量試験法を用いることができることを追記した．また，あらかじめ対象となる残留溶媒に分析に適した方法を設定することが必要であることを明記し，状況に応じた対応が重要であることを示した．さらに，医薬品各条には残留溶媒の規格は設定しない方向にあるが，これは残留溶媒は医薬品の製造方法に依存するために一律に設定できないためであり，残留溶媒の管理は，医薬品の製造工程でどのような溶媒を使ったかにより各製造業者が残留量を適切に把握し，自主的に管理する必要があることを追記した．これらは，日局17に向けた下準備のための記載整備といえる．なお，連動して参考情報の残留溶媒も一部加筆修正した．

プラスチック製医薬品容器試験法 —ポリ塩化ビニル製水性注射剤容器—

ポリ塩化ビニル製水性注射剤容器の(11)塩化ビニルの試験法のなかで，日局15では，2つの分析条件のガスクロマトグラフィーが記載されており，塩化ビニルモノマーの標準液のピークより大きなピークがいずれか一方の測定条件で認められなければ試験に合格するという変則的な試験法で，判定法が不明瞭であったため，記載を整備した．

その後，この日局15の試験方法が，塩化ビニル容器の試料を完全に溶解して，パックドカラムのガスクロマトグラフィーに注入するというもので，妨害成分の影響が大きく，カラムの汚染が激しいために，カラムの空焼きに長時間を要するなどの問題点があった．そこで日局16では，食品，添加物などの規格基準の塩化ビニル試験法を基に，キャピラリーカラムを使用して，試料を*N*,*N*-ジメチルアセトアミド(DMA)を溶媒として溶解させ，マニュアルサンプリングによるヘッドスペース法により注入後，水素炎イオン化検出器で検出する方法へ変更した．

導電率測定法

水の各条改正に伴い，試験に用いる水の記載を変更した．「蒸留水又は精製水(導電率2 μS・cm^{-1}以下)」となっていたものを，「蒸留水又は導電率2 μS・cm^{-1}以下の水」へ変更し，精製水という用語を使用しない方向へ統一した．同様に，pH測定法でも，「精製水を蒸留し，留液を15分間以上煮沸した後，」となっていたのを，「蒸留した水を15分間以上煮沸した後，」へと変更した．

さらに，塩化カリウム標準溶液の測定が20℃で行えない場合の温度補正式の有効範囲を，20±5℃から，15～30℃へ広げた．これは水の導電率測定が25℃でなされることとなっており，測定温度での校正を可能とするためである．

なお，導電率測定法は国際調和の対象となっている試験法であるが，日局16に記載されている塩化カリウム標準溶液の導電率はJISなどに収載されている値と若干異なっており，早期の改正が待たれている．

参考情報，近赤外吸収スペクトル測定法

医薬品の最終製品の品質を保証することを目的として，製造プロセスにおける重要な品質特性を連続的に計測管理する手法であるPAT (Process Analytical technology) が欧米で推進されており，わが国でも品質の管理手法として取り込まれるようになってきている．PATの代表的な分析ツールとして，近赤外吸収スペクトルがあり，非破壊測定，連続測定，多成分同時測定が可能で，すでにUSP

やEPで一般試験法として設定されている．日局では，第二追補に参考情報として収載された．

近赤外吸収スペクトルでは，750～2,500nmの波長の近赤外光の吸収を測定し，主に水素結合が関与するO-H，N-H，C-Hなどに由来する吸収が捉えられる．近赤外分光光度計として，分散型近赤外分光光度計およびフーリエ型近赤外分光光度計が主に医薬品分野で使用されている．測定法としては，赤外スペクトルと同様に，試料の形状に応じて，透過法，拡散反射法，透過反射法の測定法を選択する．装置性能の管理では，波長の精度の確認など詳細に記載されており，定性または定量分析への応用に関しても概説されている．

参考情報，誘導結合プラズマ発光分光分析法

医薬品の金属元素などの無機性不純物などの測定法としては，すでに一般試験法として原子吸光光度法が収載されているが，多くの元素について同時に微量分析が可能なこと，化学的干渉による妨害がほとんどないことなどから，誘導結合プラズマ(ICP)発光分光分析法の局方への取り込みが要望されていた．ICP発光分析法は，高周波誘導結合法により得られるアルゴンプラズマ中に試料を噴霧導入し，高温の熱エネルギーにより励起された原子による発光スペクトルの波長及び強度を測定して，定性，定量分析を行うものである．

別に，ICPをイオン源とするICP質量分析法もあり，多くの部分が共通する部分も多いため，今後両者を併せた形で，一般試験法への収載を検討中である．

現在，ICH（日米欧医薬品規制調和国際会議）の場で，金属不純物の規制に関する国際調和が進行中であり，関連する個別金属の測定法も局方として取り入れる予定となっており，ICP発光分析法，ICP質量分析法が国際的に共通のツールとして取り上げられるため，今後，重要な役割を果たすことになる．

おわりに

理化学試験法では，局方の国際調和の案件としては，従来から継続しているものとして，色の試験法，導電率測定法があり現在進行中である．色の測定法では，色の標準液が局方間で異なるため，色差計による測定法の導入が検討されている．また，医薬品分析ではもっとも多用されているクロマトグラフィーの国際調和が開始されることになり，現在，わが国の医薬品の承認申請や，局方への取り込み時に生じている，試験法設定方法の差異に起因するトラブルの解消が期待されている．

The Journal of Toxicological Sciences (J. Toxicol. Sci.)
Vol.36, No.6, 725-731, 2011

Original Article

Comparison of selenoneine found in marine organisms with selenite in the interaction with mercury compounds *in vitro*

Yasumi Anan[1], Shinsuke Tanabe[2] and Yasumitsu Ogra[1,3]

[1]*Laboratory of Chemical Toxicology and Environmental Health, Showa Pharmaceutical University, 3-3165 Higashi-Tamagawagakuen, Machida, Tokyo 194-8543, Japan*
[2]*Center for Marine Environmental Studies (CMES), Ehime University, 2-5 Bunkyo-cho, Matsuyama, Ehime 790-8577, Japan*
[3]*High Technology Research Center, Showa Pharmaceutical University, 3-3165 Higashi-Tamagawagakuen, Machida, Tokyo 194-8543, Japan*

(Received August 23, 2011; Accepted September 9, 2011)

ABSTRACT — Selenium (Se) is an essential micronutrient because it forms the active center of selenoenzymes/selenoproteins in the form of selenocysteine. Another biological significance of Se is that it detoxifies inorganic mercury (iHg) by directly interacting with it. Recently, a novel selenometabolite, selenoneine (2-selenyl-*N,N,N*-trimethyl-L-histidine), was identified in several marine animals. However, its biological significance is still unclear. In this study, the ability of selenoneine to form a complex with iHg and methyl Hg (MeHg) was evaluated *in vitro*. Whereas selenite serving as the positive control reacted with iHg by direct interaction after being converted into selenide by endogenous reductants, such as glutathione (GSH), selenoneine did not interact with iHg or MeHg in the liver homogenate of marine turtle. This indicates that selenoneine may not play a role in the detoxification of Hg.

Key words: Selenoneine, Selenite, Mercury, Sea turtle, HPLC-ICP-MS

INTRODUCTION

Selenium (Se) is an essential micronutrient in animals because it promotes the activities of various enzymes, such as glutathione peroxidases, iodothyronine 5'-deiodinase, and thioredoxin reductase, by virtue of its incorporation as selenocysteine (SeCys) into their active centers (Lu and Holmgren, 2009; Reeves and Hoffmann, 2009). Proteins containing SeCys are called selenoproteins, whereas proteins containing selenomethionine (SeMet) are considered to be selenium-containing proteins due to the non-specific substitution in its sulfur analogue, methionine.

Although it is known that all Se species ingested via food and drinking water are first transformed into selenide and selenide is then utilized for the biosynthesis of SeCys for incorporation into selenoproteins, the bioavailability and metabolic pathways differ depending on the ingested chemical form. One inorganic Se, selenite, is simply reduced to selenide by endogenous reductants, such as glutathione (GSH) (Kobayashi *et al.*, 2001). Another inorganic Se, selenate, is not reduced to selenide by GSH *in vitro*, but is also utilized for selenoprotein biosynthesis *in vivo* (Shiobara *et al.*, 1999). On the other hand, organic selenocompounds ingested via food are mostly selenoamino acids, *e.g.*, SeCys, Se-methylselenocysteine (MeSeCys), and SeMet, which are transformed into selenide via different pathways, as has been mentioned in several reviews (Gammelgaard *et al.*, 2011; Ogra and Anan, 2009; Tsuji *et al.*, 2009). Hence, even though any Se species are ingested via food and drinking water, Se is utilized for selenoprotein biosynthesis and excreted as a common urinary metabolite, *i.e.*, 1ß-methylseleno-*N*-acetyl-D-galactosamine, at physiological and low toxicity levels, and as trimethylselenonium (TMSe) when excess amounts of Se are ingested (Suzuki *et al.*, 2005).

Another biological significance of Se is that it detoxifies inorganic mercury (iHg) by directly interacting with it. The administration of selenite at a lethal dose antagonized the lethal dose of iHg in experimental animals (Naganuma *et al.*, 1984; Su *et al.*, 2008; Yoneda and Suzuki, 1997). Good positive correlation was noted between Se and Hg concentrations in the livers of marine mammals and seabirds, which highly accumulated Hg in their liv-

Correspondence: Yasumitsu Ogra (E-mail: ogra@ac.shoyaku.ac.jp)

ers (Kim *et al.*, 1996; Storelli *et al.*, 1998; Woshner *et al.*, 2001). Hg and Se at an equimolar ratio formed a complex (mercury selenide, tiemannite) that was accumulated in the livers of marine animals. Although the mechanism for the complex formation is still unclear, the following is speculated (Ikemoto *et al.*, 2004). Methyl mercury (MeHg) in food is demethylated after ingestion and then, iHg is bound to proteins. Se is also bound to proteins in the form of selenide via the metabolic pathway mentioned above regardless of the Se species ingested. The proteins that bind iHg and Se are transported to lysosomes for degradation. Consequently, the Hg-Se complex may be formed upon the degradation of proteins in lysosomes.

Recently, a novel selenometabolite, selenoneine (2-selenyl-*N,N,N*-trimethyl-L-histidine), was identified in bluefin tuna and other fish species (Yamashita and Yamashita, 2010). It is also reported that sea turtles accumulate Se in their livers in spite of the low hepatic Hg concentration, and the major portion of Se in the liver exists as selenoneine (Anan *et al.*, 2011). On the other hand, selenoneine in the liver of terrestrial turtle was below the detection limit (Anan *et al.*, 2011). These suggest that selenoneine is transferred among marine organisms via the food web to result in its ubiquitous distribution in the marine ecosystem. However, the origin and the biological significance of selenoneine are yet unclear. In addition, the role of selenoneine in the detoxification of Hg is also not evident.

In this study, the ability of selenoneine to form a complex with iHg and MeHg was evaluated *in vitro*. As the source of selenoneine, the liver of hawksbill turtle (*E. imbricata*) with low endogenous Hg was used. In addition, ^{82}Se-labeled selenite was used as the positive control for the formation of the Hg-Se complex. The utilization of an enriched Se stable isotope allowed us to directly and simultaneously compare the interaction of Se compounds with Hg in biological samples. Finally, the role of selenoneine in the detoxification of iHg and MeHg was discussed.

MATERIALS AND METHODS

Reagents

All reagents were of analytical grade or the highest grade available. Purified water (18.3 MΩ·cm) from Milli-Q SP (Millipore, Bedford, MA, USA) was used throughout. Trizma® Base and HCl were purchased from Sigma (St. Louis, MO, USA). Mercury chloride ($HgCl_2$), methylmercury chloride (CH_3HgCl), and all other chemicals were purchased from Wako Pure Chemical Industries, Ltd. (Osaka, Japan). The metallic form of ^{82}Se (98.9% enriched) was purchased from Isoflex USA, San Francisco, USA. ^{82}Se-Selenite was prepared by dissolving the metallic form of ^{82}Se in concentrated nitric acid, followed by adjustment to neutral pH with 0.1 M NaOH as previously reported (Kobayashi *et al.*, 2001).

Sample preparation and *in vitro* assay

Liver specimen of hawksbill turtle (*E. imbricata*) was provided by fishermen in the Yaeyama Islands, Okinawa, Japan. This turtle was captured in November 2000, for the commercial and scientific purposes after receiving the official permission. Following collection, the liver specimen was immediately frozen in liquid nitrogen and stored at -80°C until analyses in the Environmental Specimen Bank for Global Monitoring (es-BANK), Center for Marine Environmental Studies (CMES), Ehime University, Japan (Tanabe, 2006). The Se concentration in this sample was determined to be 43 μg Se/g tissue in our previous study (Anan *et al.*, 2011). The liver was homogenized in ten times volume of 50 mM Tris-HCl buffer (pH 7.4, 25°C) after bubbling the buffer with nitrogen gas to purge dissolved oxygen. A 1 ml aliquot of homogenate was incubated with $HgCl_2$ at the final concentration of 1.0 μg Hg/ml at 37°C for 60 min. Another 1 ml aliquot was pre-incubated with ^{82}Se-selenite at the final concentration of 1.0 μg Se/ml at 37°C for 10 min and then incubated with $HgCl_2$ at the final concentration of 1.0 or 2.5 μg Hg/ml, CH_3HgCl at the final concentration of 2.5 μg Hg/ml, or buffer at 37°C for 60 min. The homogenates were centrifuged at 105,000 *g* for 60 min at 4°C to obtain the supernatant fraction. The procedure for the *in vitro* assay is shown in Fig. 1.

HPLC-ICP-MS analysis

An ICP-MS instrument (Agilent7500ce, Agilent Technologies, Tokyo, Japan) was coupled to an HPLC system as the detector. The HPLC system consisted of an online degasser, an HPLC pump (Prominence; Shimadzu, Kyoto, Japan), a Rheodyne six-port injector with a sample loop, and a column. A 200 μl aliquot of the supernatant was applied to a multimode gel filtration column (Shodex Asahipak GS-520 HQ, 7.5 i.d. x 300 mm, with a guard column, 7.5 i.d. x 75 mm; Showa Denko, Tokyo), and the column was eluted with 50 mM Tris-HCl, pH 7.4, at the flow rate of 0.6 ml/min. The eluate was introduced directly into the nebulizer of the ICP-MS to detect Se at *m/z* 78 and 82, Hg at *m/z* 202, Zn at *m/z* 66, and Cd at *m/z* 111 in the D_2 reaction mode (Ogra *et al.*, 2005). The distribution of exogenous selenite was calculated from the counts of ^{78}Se and ^{82}Se as previously reported (Suzuki *et al.*, 2006b).

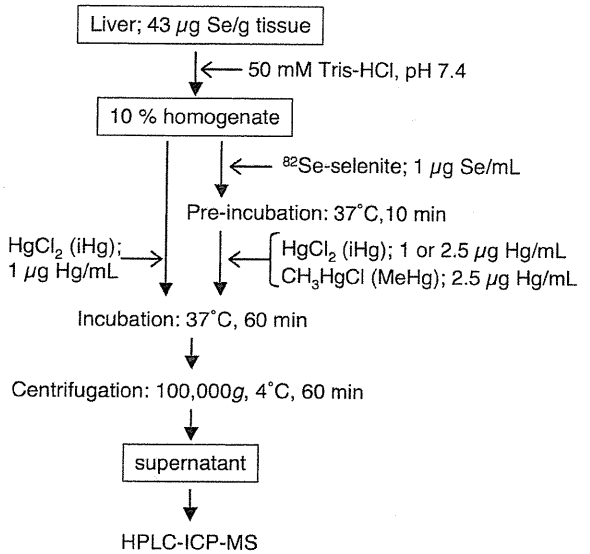

Fig. 1. Procedure for *in vitro* assay.

RESULTS AND DISCUSSION

Distribution of endogenous metals/metalloids and exogenous inorganic mercury in liver cytosol

As has been previously reported (Anan *et al.*, 2011), the major Se metabolite in the supernatant of hawksbill turtle was selenoneine, which corresponded to the peak that appeared at the retention time of 21.8 min (Fig. 2a). By magnifying the Se elution profile, a peak corresponding to methylated selenosugar (1ß-methylseleno-*N*-acetyl-D-galactosamine) was detected at the retention time of 20.7 min. In addition, several peaks of selenoproteins or selenium-containing proteins were detected at the retention times of 11-16 min, which corresponded to the high molecular weight protein fraction on the column. The Se peak at the retention time of 17.7 min coincided with the peak of endogenous Hg. The marine turtle accumulates less Hg in the liver than other marine mammals (Anan *et al.*, 2001). However, the results indicated that a trace amount of endogenous Se and Hg formed a complex and the complex was bound to high molecular weight molecule(s) in the liver of hawksbill turtle. No apparent changes in the selenoneine peak were observed by the addition of iHg (Fig. 2b). This suggests that selenoneine is not able to react with iHg in the liver homogenate *in vitro*.

A trace amount of endogenous Hg was detected and found to bind to some high molecular weight molecules. Exogenous iHg was mainly distributed to the two peaks that appeared at the retention times of 13.9 and 15.5 min. Meanwhile, endogenous Zn was distributed to the same peaks as those of exogenous Hg, whereas endogenous Cd was bound to only the latter peak. Furthermore, the intensity of the endogenous Zn that corresponded to the latter peak was decreased by the addition of iHg. These results indicate that the latter peak corresponds to metal-binding protein, e.g. metallothionein (MT). MT can bind Hg, Zn, and Cd with different affinities, i.e., the order of affinity is Hg ≥ Cd > Zn (Eaton, 1985; Waalkes *et al.*, 1984). Thus, it was most likely that the amount of endogenous Zn bound to MT was decreased because endogenous Zn was replaced with exogenous iHg in MT *in vitro*. A portion of Zn that bound to other Zn binding protein(s) at the retention time of 13.9 min was partially substituted with exogenous iHg.

Interaction of inorganic and methylated Hg with [^{82}Se]-selenite in liver of hawksbill turtle

The utilization of ^{82}Se-labeled selenite (exogenous selenite) allowed us to directly compare the ability of selenite and selenoneine to interact with Hg in the liver of hawksbill turtle *in vitro*. The elution profiles of ^{78}Se and ^{82}Se showed the distributions of endogenous Se and endogenous plus exogenous Se, respectively. The elution profile of exogenous Se was depicted by calculations made on the basis of the counts of ^{78}Se and ^{82}Se. Although authentic selenite was eluted at the retention time of 18.3 min, no Se peaks were detected at that retention time (Fig. 3, middle panel), indicating that exogenous Se was converted into other chemical species in the liver homogenate. Exogenous Se was distributed to the protein fractions and the low molecular weight compound(s) whose peaks appear at the retention times of 11-15 min and 16.5 min, respectively (Fig. 3a, middle panel). As reported previously, selenite is easily reduced to selenide by such endogenous reductants as GSH in the liver and then selenide is bound to proteins and GSH due to its reactivity with the sulfhydryl group (Suzuki *et al.*, 2006a). Thus, the Se peaks appearing at the retention times of 11-15 min and 16.5 min may be protein-bound and GSH-conjugated selenide, respectively. The peak at the retention time of 21.8 min corresponded to selenoneine. However, that peak seemed to be noise resulting from the calculation.

Exogenous Hg at the concentration of 1.0 μg/ml decreased the intensity of the Se peak corresponding to GSH-conjugated Se species, and Hg was co-eluted with exogenous Se at the retention times of 11-15 min on the chromatogram (Fig. 3b). These suggest that exogenous

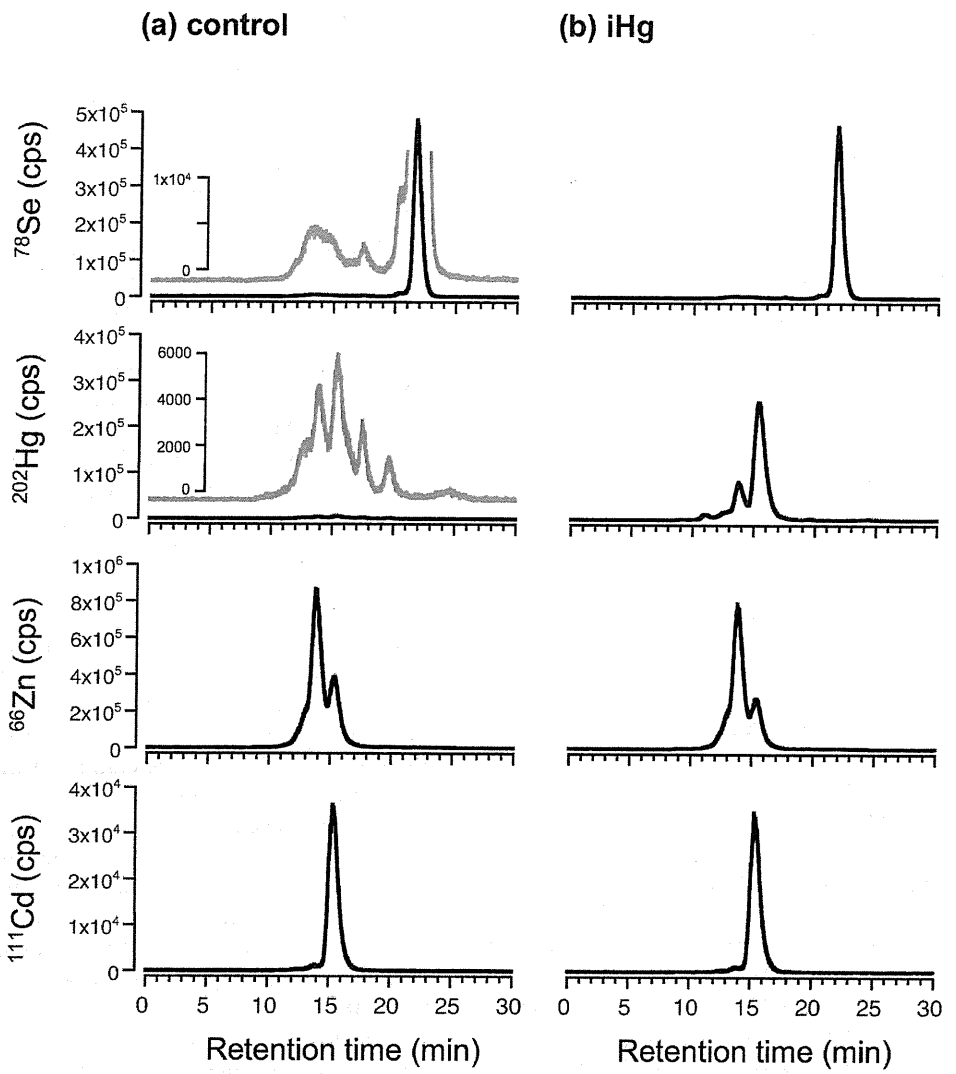

Fig. 2. Elution profiles of ^{78}Se, ^{202}Hg, ^{66}Zn, and ^{111}Cd in the supernatant obtained from control liver homogenate (a) and that incubated with inorganic Hg (iHg) (b). Gray lines show the magnified elution profiles.

Hg formed complex(es) with exogenous Se, i.e., selenide, and the complex(es) were distributed to the high molecular weight protein fraction. It was reported that the Se-Hg complex was specifically bound to selenoprotein P (Sel P) in the bloodstream of a whole animal (Suzuki *et al.*, 1998). Although Sel P is biosynthesized in the liver, it is promptly secreted into the bloodstream after post-translational modification in the Golgi apparatus (Burk and Hill, 2009). Thus, no specific binding proteins exist in the liver homogenate. The peak area of exogenous Se was decreased by the addition of iHg at the concentration of 2.5 μg/ml, compared with that by the addition at 1.0 μg/ml (Fig. 3c). This means that the addition of an excess amount of iHg induces to insolubilize the Se-Hg complex. The excess amount of iHg that did not react with selenide was eluted at the retention time of 15.5 min (Fig. 3c, bottom panel). Clearly, free iHg was re-bound to MT.

Contrary to the reactivity of selenide with iHg, selenoneine was inert to the addition of iHg even at a high concentration. This suggests that selenoneine is not involved in the detoxification of Hg.

When methyl mercury (MeHg) was added to the liver homogenate with exogenous selenite, Hg was mainly distributed to the protein fraction (Fig. 4, bottom panel).

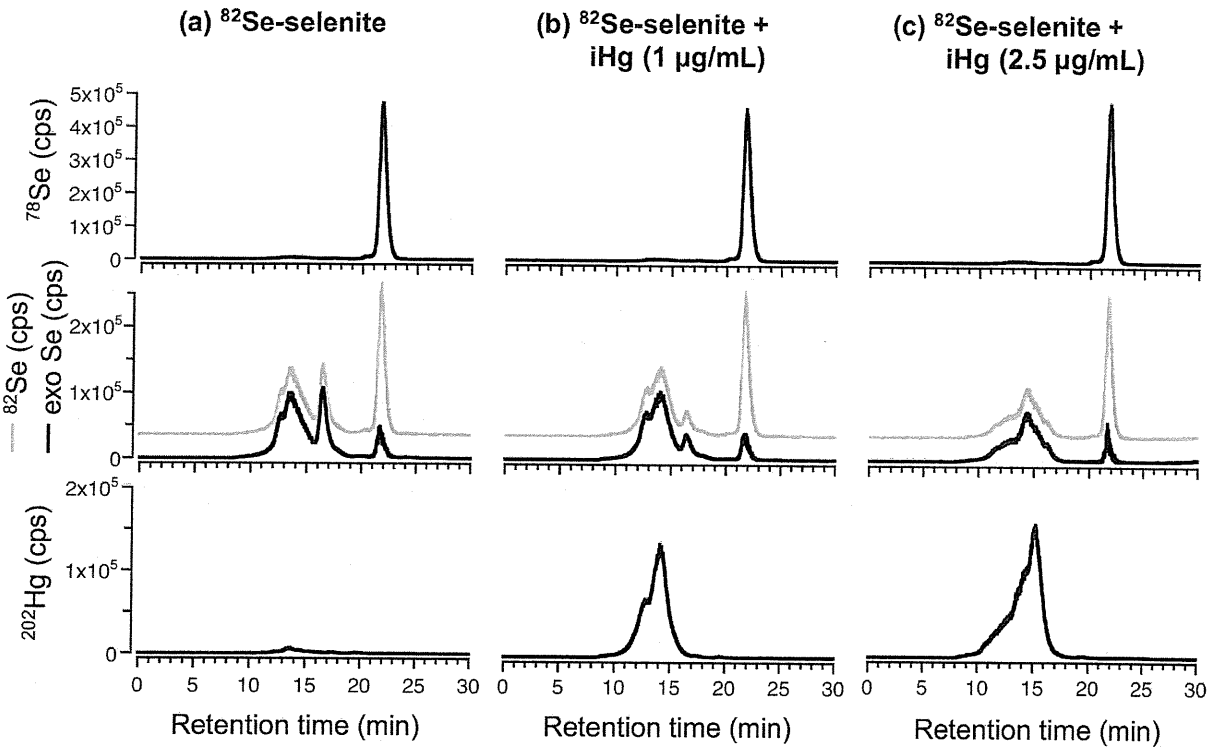

Fig. 3. Elution profiles of ^{78}Se, ^{82}Se, and ^{202}Hg in the supernatant obtained from homogenate incubated with ^{82}Se selenite (a), ^{82}Se-selenite plus inorganic Hg (iHg) at the concentration of 1.0 µg Hg/ml (b), and ^{82}Se-selenite plus iHg at the concentration of 2.5 µg Hg/ml (c). Exogenous Se (exo Se) was calculated by subtraction of endogenous ^{82}Se from total ^{82}Se count.

There were no apparent changes in the Se distribution in the supernatant (Figs. 3a and 4). Although the intensity of the peak corresponding to GSH-conjugated Se was obviously decreased with the addition of iHg, GSH-conjugated Se did not seem to interact with MeHg. Many studies have revealed that selenite is able to alleviate MeHg toxicity *in vivo* (Carvalho *et al.*, 2011; Glaser *et al.*, 2010; Heath *et al.*, 2010). MeHg exhibits toxicity by inhibiting selenoenzyme activity and protein syntheses, and generating reactive oxygen species (ROS). It is reported that selenite can boost the activities of selenoenzymes and scavenge ROS (Glaser *et al.*, 2010). Thus, selenite may indirectly mitigate the toxic effects of MeHg *in vivo* despite the fact that selenide originating from selenite does not directly interact with MeHg *in vitro*. Meanwhile, it is reported that MeHg ingested is partially degraded into iHg *in vivo* (Havarinasab *et al.*, 2007) and thus, it may react with selenide as iHg. The peak corresponding to selenoneine was not affected by MeHg, suggesting that selenoneine did not interact with MeHg *in vitro*. Consequently, the biosynthesis of selenoneine is independent of the defense mechanism against Hg toxicity in marine fish and reptiles.

In conclusion, although selenite is one of the detoxification factors of iHg and acts by directly interacting with iHg after its conversion to selenide by endogenous reductants, such as GSH, selenoneine does not interact with iHg and MeHg at least in the liver of marine turtle. Thus, selenoneine may not act as the detoxification factor of Hg. MT is another detoxification factor because it actually sequesters iHg. It has reported that selenoneine shows the antioxidant activity *in vitro* (Yamashita and Yamashita, 2010). Recently, methylated selenoneine was detected in human urine (Klein *et al.*, 2011). These suggest that the selenone moiety in selenoneine is physiologically and biologically active because it is masked with a methyl group as a metabolite. Further studies are needed to reveal the physiological and/or toxicological significance of selenoneine in marine animals.

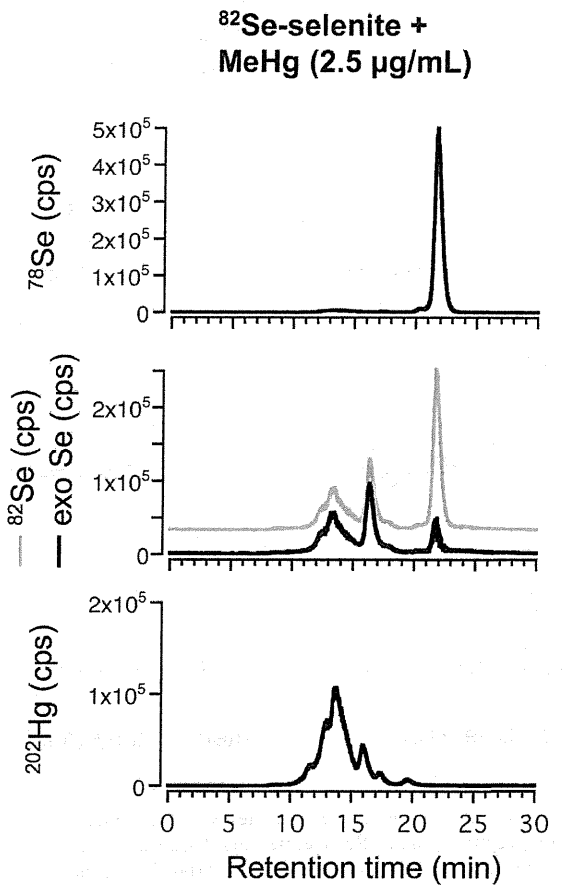

Fig. 4. Elution profiles of ^{78}Se, ^{82}Se, and ^{202}Hg in the supernatant obtained from liver homogenate incubated with ^{82}Se-selenite plus methyl Hg (MeHg). Exogenous Se (exo Se) was calculated by subtraction of endogenous ^{82}Se from total ^{82}Se count.

ACKNOWLEDGMENTS

The authors wish to thank Dr. N. Kamezaki, Mr. T. Shima, Mr. M. Wakatsuki, and Mr. S. Yamashiro for their help in the collection of samples. This study was supported by a Grant-in-Aid from the Ministry of Education, Culture, Sports, Science and Technology, Japan (No. 23390032 to Y.O.), and a financial support from Agilent Technologies Foundation, USA.

REFERENCES

Anan, Y., Ishiwata, K., Suzuki, N., Tanabe, S. and Ogra, Y. (2011): Speciation and identification of low molecular weight selenium compounds in the liver of sea turtles. J. Anal. At. Spectrom., **26**, 80-85.

Anan, Y., Kunito, T., Watanabe, I., Sakai, H. and Tanabe, S. (2001): Trace element accumulation in hawksbill turtles (*Eretmochelys imbricata*) and green turtles (*Chelonia mydas*) from Yaeyama Islands, Japan. Environ. Toxicol. Chem., **20**, 2802-2814.

Burk, R.F. and Hill, K.E. (2009): Selenoprotein P-expression, functions, and roles in mammals. Biochim. Biophys. Acta, **1790**, 1441-1447.

Carvalho, C.M., Lu, J., Zhang, X., Arnér, E.S. and Holmgren, A. (2011): Effects of selenite and chelating agents on mammalian thioredoxin reductase inhibited by mercury: implications for treatment of mercury poisoning. FASEB J., **25**, 370-381.

Eaton, D.L. (1985): Effects of various trace metals on the binding of cadmium to rat hepatic metallothionein determined by the Cd/hemoglobin affinity assay. Toxicol. Appl. Pharmacol., **78**, 158-162.

Gammelgaard, B., Jackson, M.I. and Gabel-Jensen, C. (2011): Surveying selenium speciation from soil to cell--forms and transformations. Anal. Bioanal. Chem., **399**, 1743-1763.

Glaser, V., Nazari, E., Müller, Y.M., Feksa, L., Wannmacher, C.M., Rocha, J.B., de Bem, A.F., Farina, M. and Latini, A. (2010): Effects of inorganic selenium administration in methylmercury-induced neurotoxicity in mouse cerebral cortex. Int. J. Dev. Neurosci., **28**, 631-637.

Havarinasab, S., Björn, E., Nielsen, J.B. and Hultman, P. (2007): Mercury species in lymphoid and non-lymphoid tissues after exposure to methyl mercury: correlation with autoimmune parameters during and after treatment in susceptible mice. Toxicol. Appl. Pharmacol., **221**, 21-28.

Heath, J.C., Banna, K.M., Reed, M.N., Pesek, E.F., Cole, N., Li, J. and Newland, M.C. (2010): Dietary selenium protects against selected signs of aging and methylmercury exposure. Neurotoxicology, **31**, 169-179.

Ikemoto, T., Kunito, T., Tanaka, H., Baba, N., Miyazaki, N. and Tanabe, S. (2004): Detoxification mechanism of heavy metals in marine mammals and seabirds: interaction of selenium with mercury, silver, copper, zinc, and cadmium in liver. Arch. Environ. Contam. Toxicol., **47**, 402-413.

Kim, E.Y., Saeki, K., Tanabe, S., Tanaka, H. and Tatsukawa, R. (1996). Specific accumulation of mercury and selenium in seabirds. Environ. Pollut., **94**, 261-265.

Klein, M., Ouerdane, L., Bueno, M. and Pannier, F. (2011): Identification in human urine and blood of a novel selenium metabolite, Se-methylselenoneine, a potential biomarker of metabolization in mammals of the naturally occurring selenoneine, by HPLC coupled to electrospray hybrid linear ion trap-orbital ion trap MS. Metallomics, **3**, 513-520.

Kobayashi, Y., Ogra, Y. and Suzuki, K.T. (2001): Speciation and metabolism of selenium injected with 82Se-enriched selenite and selenate in rats. J. Chromatogr. B Biomed. Sci. Appl., **760**, 73-81.

Lu, J. and Holmgren, A. (2009): Selenoproteins. J. Biol. Chem., **284**, 723-727.

Naganuma, A., Ishii, Y. and Imura, N. (1984): Effect of administration sequence of mercuric chloride and sodium selenite on their fates and toxicities in mice. Ecotoxicol. Environ. Saf., **8**, 572-

580.

Ogra, Y. and Anan, Y. (2009): Selenometabolomics: Identification of selenometabolites and specification of their biological significance by complementary use of elemental and molecular mass spectrometry. J. Anal. At. Spectrom., **24**, 1477-1488.

Ogra, Y., Ishiwata, K. and Suzuki, K.T. (2005): Effects of deuterium in octopole reaction and collision cell ICP-MS on detection of selenium in extracellular fluids. Anal. Chim. Acta, **554**, 123-129.

Reeves, M.A. and Hoffmann, P.R. (2009): The human selenoproteome: recent insights into functions and regulation. Cell Mol. Life Sci., **66**, 2457-2478.

Shiobara, Y., Ogra, Y. and Suzuki, K.T. (1999): Speciation of metabolites of selenate in rats by HPLC-ICP-MS. Analyst, **124**, 1237-1241.

Storelli, M.M., Ceci, E. and Marcotrigiano, G.O. (1998): Comparison of total mercury, methylmercury, and selenium in muscle tissues and in the liver of Stenella coeruleoalba (Meyen) and Caretta caretta (Linnaeus). Bull. Environ. Contam. Toxicol., **61**, 541-547.

Su, L., Wang, M., Yin, S.T., Wang, H.L., Chen, L., Sun, L.G. and Ruan, D.Y. (2008): The interaction of selenium and mercury in the accumulations and oxidative stress of rat tissues. Ecotoxicol. Environ. Saf., **70**, 483-489.

Suzuki, K.T., Kurasaki, K., Okazaki, N. and Ogra, Y. (2005): Selenosugar and trimethylselenonium among urinary Se metabolites: dose- and age-related changes. Toxicol. Appl. Pharmacol., **206**, 1-8.

Suzuki, K.T., Sasakura, C. and Yoneda, S. (1998): Binding sites for the (Hg-Se) complex on selenoprotein P. Biochim. Biophys. Acta, **1429**, 102-112.

Suzuki, K.T., Somekawa, L., Kurasaki, K. and Suzuki, N. (2006a): Absolute Labeling and Simultaneous Speciation in Tracer Experiments with Multiple Stable Isotopes. J. Health Sci. **52**, 590-597.

Suzuki, K.T., Somekawa, L., Kurasaki, K. and Suzuki, N. (2006b): Simultaneous tracing of 76Se-selenite and 77Se-selenomethionine by absolute labeling and speciation. Toxicol. Appl. Pharmacol., **217**, 43-50.

Tanabe, S. (2006): Environmental Specimen Bank in Ehime University (es-BANK), Japan for global monitoring. J. Environ. Monit., **8**, 782-790.

Tsuji, Y., Suzuki, N., Suzuki, K.T. and Ogra, Y. (2009): Selenium metabolism in rats with long-term ingestion of Se-methylselenocysteine using enriched stable isotopes. J. Toxicol. Sci., **34**, 191-200.

Waalkes, M.P., Harvey, M.J. and Klaassen, C.D. (1984): Relative *in vitro* affinity of hepatic metallothionein for metals. Toxicol. Lett., **20**, 33-39.

Woshner, V.M., O'Hara, T.M., Bratton, G.R., Suydam, R.S. and Beasley, V.R. (2001). Concentrations and interactions of selected essential and non-essential elements in bowhead and beluga whales of arctic Alaska. J. Wildl. Dis., **37**, 693-710.

Yamashita, Y. and Yamashita, M. (2010): Identification of a novel selenium-containing compound, selenoneine, as the predominant chemical form of organic selenium in the blood of bluefin tuna. J. Biol. Chem., **285**, 18134-18138.

Yoneda, S. and Suzuki, K.T. (1997): Detoxification of mercury by selenium by binding of equimolar Hg-Se complex to a specific plasma protein. Toxicol. Appl. Pharmacol., **143**, 274-280.

Metallomics

Dynamic Article Links

Cite this: *Metallomics*, 2011, **3**, 693–701

www.rsc.org/metallomics

PAPER

Roles of copper chaperone for superoxide dismutase 1 and metallothionein in copper homeostasis†

Takamitsu Miyayama,[a] Yudai Ishizuka,[a] Tomomi Iijima,[a] Daisuke Hiraoka[b] and Yasumitsu Ogra*[ac]

Received 29th January 2011, Accepted 22nd February 2011
DOI: 10.1039/c1mt00016k

Copper chaperone for SOD1 (CCS) specifically delivers copper (Cu) to copper, zinc superoxide dismutase (SOD1) in cytoplasm of mammalian cells. In the present study, small interfering RNA (siRNA) targeting CCS was introduced into metallothionein-knockout mouse fibroblasts (MT-KO cells) and their wild type cells (MT-WT cells) to reveal the interactive role of CCS with other Cu-regulating proteins, in particular, MT. CCS knockdown significantly decreased Ctr1, a Cu influx transporter, mRNA expression. On the other hand, Atp7a, a Cu efflux transporter, mRNA expression was increased 3.0 and 2.5 times higher than those of the control in MT-WT and MT-KO cells. These responses of Cu-regulating genes to the CCS knockdown reflected the presence of excess Cu in the cells. To evaluate the Atp7a function in the Cu-replete cells, siRNA of Atp7a and the other Cu transporter, Atp7b were introduced into MT-WT and MT-KO cells. The Atp7a knockdown significantly increased the intracellular Cu concentration, whereas the Atp7b knockdown had no affect. Although two MT isoforms were induced by the CCS knockdown in MT-WT cells, the expression and activity of SOD1 were maintained in both MT-WT and MT-KO cells even when CCS protein expression was reduced to 0.30–0.35 of control. This suggests that the amount of CCS protein exceeds that required to supply Cu to SOD1 in the cells. Further, the CCS knockdown induces Cu accumulation in cells, however, the Cu accumulation is ameliorated by the MT induction, the decrease of Ctr1 expression and the increase of Atp7a expression to maintain Cu homeostasis.

Introduction

Copper (Cu) is an essential trace element in all living organisms. It forms the active center of cuproenzymes, such as Cu, zinc (Zn)-superoxide dismutase (Cu, Zn-SOD, SOD1), cytochrome c oxidase (CCO), ceruloplasmin, lysyl oxidase, tyrosinase, and dopamine β-hydroxylase.[1] The function of Cu in the cuproenzymes is to facilitate the transition between cuprous (monovalent) and cupric (divalent) oxidation states. Harmful reactive oxygen species may be generated if free Cu ion exists in cells by this chemical property. Therefore, cells have strictly controlled mechanisms for the incorporation, intracellular distribution, utilization, and excretion of Cu. The mechanisms underlying Cu distribution to these cuproenzymes are suggested as follows.[2] Cu is mainly incorporated into cells as cuprous ion by Ctr1, a transporter expressed on the plasma membrane.[3,4] The incorporated Cu associates with one of three cytoplasmic Cu escort proteins, the so-called Cu chaperones, for distribution to specific organelles or cuproenzymes. It is known that the Cu chaperone for SOD1 (abbreviated as CCS) hands over Cu to SOD1 in cytosol by forming a heterodimer with SOD1. Indeed, CCS-knockout mice showed similar clinical manifestations to SOD1-knockout mice such as decreased SOD1 activity and enhanced sensitivity to oxidative stress. However, the CCS-KO mice SOD1 activity remains at 10–20% in all tissues except the liver, and 30% in the liver in spite of the lack of CCS.[5] This suggests that SOD1 requires Cu supplementation by not only CCS but also the other Cu binding proteins to display its activity. The second Cu chaperone, Atox1, delivers Cu to Atp7a and Atp7b, which are ATP-dependent Cu transporters into the secretory pathway of Cu *via* the Golgi apparatus.[6,7] In the Golgi apparatus, Cu is incorporated into such cuproenzymes as ceruloplasmin and lysyl oxidase, due to the secretion of these cuproenzymes into the extracellular fluid. Otherwise, Cu is directly effluxed from the cells by secretory vesicles that translocate from the trans Golgi

[a] *Laboratory of Chemical Toxicology and Environmental Health, Showa Pharmaceutical University, 3-3165 Higashi-Tamagawagakuen, Machida, Tokyo 194-8543, Japan. E-mail: ogra@ac.shoyaku.ac.jp; Fax: +81 42 721 1563; Tel: +81 42 721 1563*
[b] *Graduate School of Pharmaceutical Sciences, Chiba University, Chuo, Chiba 260-8675, Japan*
[c] *High Technology Research Center, Showa Pharmaceutical University, Machida, Tokyo 194-8543, Japan*

† This article is published as part of a themed issue highlighting metallomics research in Japan, including contributions from the 2nd Metallomics Research Forum, Kyoto, Japan, held on 2nd–3rd November 2010. This issue is guest edited by Hiroki Haraguchi and Hiroyuki Yasui.

membrane to the plasma membrane to excrete Cu. The third Cu chaperone, Cox17, a Cu chaperone for mitochondria, is required to donate Cu to CCO and/or SCO1, a recipient protein of Cu on the mitochondrial membrane.[8,9]

In addition to these Cu chaperones, metallothionein (MT) is suggested to be also a Cu-regulating protein. MT is a cysteine-rich low molecular weight protein. Because it possesses abundant mercaptide bonds, MT actually binds Cu *via* Cu-thiolate clusters.[10] As the binding of Cu by MT is thermodynamically and kinetically stable, excess Cu is sequestered by MT to mask Cu toxicity.[11] On the other hand, an alleviative role of MT in Cu deficiency was also suggested.[12,13] In our previous work, we noted that MT-null cells established from MT-knockout mouse fibroblasts (MT-KO cells) were more sensitive to the Cu-deficient condition induced by a cuprous-ion-specific chelator, bathocuproine sulfonate (BCS), than MT-wild type (MT-WT) cells.[12] Thus, MT may play a dual role in maintaining Cu homeostasis in mammalian cells under both excess Cu and Cu-deficient conditions.

As mentioned above, the functions of individual Cu-regulating proteins, such as membrane transporters, chaperones in the cytoplasm, and MT, have been clarified. However, the interactive roles, *i.e.*, crosstalk among Cu-regulating proteins, remain unclear. For instance, as regards the direct interaction between MT and SOD1, it was revealed that MT was able to directly donate Cu to SOD1 *in vitro*, similar to CCS.[14] Atox1 knockdown induced Cu accumulation in the cells and the accumulated Cu could be detoxified by cytoplasmic vesicles in place of MT in MT-KO cells.[15] Although Cu was accumulated by the Atox1 knockdown in both MT-WT and MT-KO cells, cells bearing Atox1 knockdown and MT-null mutation showed responses to Cu deficiency, such as decreases in Ctr1 expression and Atp7b expression.[16] This phenomenon could be explained as follows: elevated Cu was detoxified by compartmentalization and Cu compartmentalized in the vesicles might be less bioavailable than Cu bound to MT. These observations suggest that Cu-regulating proteins cooperatively and strictly regulate Cu homeostasis.

In the present study, we focus on the interactive roles of CCS with other Cu-regulating proteins, in particular, MT. Small interfering (siRNA) targeting CCS was introduced into MT-WT and MT-KO cells and the expression of Cu-regulating factors, SOD1 activity, and the content and distribution of Cu were determined. In addition, although MT-WT and MT-KO cells established from fibroblasts of MT-WT and MT-null mice, respectively, express both Atp7a and Atp7b, it is still unclear why two functionally similar Cu transporters are expressed in the cells. Hence, the differences between Atp7a and Atp7b in the contribution to the Cu efflux were quantitatively clarified by the Cu determination in either Atp7a or Atp7b knockdown cells by an inductively coupled plasma mass spectrometry (ICP-MS).

Materials and methods

Cell culture

MT-WT and MT-KO cells were established from embryonic fibroblasts of 129Sv MT-WT and MT-KO mice transformed with SV40 large T antigen by Kondo *et al.*[17] and kindly provided by Professor Seiichiro Himeno (Tokushima Bunri University, Japan). Cells were maintained in Dulbecco's modified Eagle's medium (DMEM) of the high glucose type (4500 mg L^{-1}) and supplemented with 10% heat inactivated fetal bovine serum, 10 U mL^{-1} penicillin, and 100 μg mL^{-1} streptomycin at 37 °C under 5% CO_2 atmosphere.

Gene knockdown

Double-stranded RNAs (dsRNAs) were used as siRNAs (Stealth™ RNAi, Invitrogen). The targeted sequence of CCS (5′–UACUGAUGCACAUGGAGUCCAUGCA–3′), Atp7a (5′–UACCAAUGAGGACUUUGUACUGCUG–3′) and Atp7b (5′–CGUCUGUCAUGAACCUGCAGCAGAU–3′) were designed from the mouse CCS (Genbank™ accession number NM_016892), Atp7a (NM_009726), Atp7b (NM_007511) genes sequence. MT-WT and MT-KO cells were seeded on a 6-well plastic plate at 2.0×10^5 cells/well and pre-incubated for 24 h. The pre-incubated cells were transfected with 100 nM siRNA targeting CCS or control siRNA in the medium optimized for siRNA transfection (Opti-MEM®I, Invitrogen) containing 1.0% Lipofectamine™ 2000 (Invitrogen) for 24 h.

Western blotting

Cells were lysed in phosphate buffered saline (PBS) containing 1% Triton X-100, 0.1% SDS, 1 mM EDTA, and a cocktail of protease inhibitors (Hoffmann-La Roche Ltd., Basel, Switzerland) for 1 h on ice. The supernatant was obtained by centrifugation of the lysate for 20 min at 16000 *g* at 4 °C.[17] The protein samples were electrophoresed through 12.5% polyacrylamide gel and transferred to a PVDF membrane at 20 V for 20 min. The membrane was blocked overnight with 5% skim milk in 25 mM Tris-HCl containing 0.9% NaCl and 0.05% Tween 20, pH 7.5 (TBS-T) at 4 °C, incubated with anti-CCS (1 : 2500 diluted) or anti-SOD1 (1 : 2000) in TBS-T for 1 h, and washed three times with TBS-T. A synthetic peptide of the mouse CCS sequence H_2N–WEERGRPIAGQGRKDS–COOH was used as an antigen to produce an antibody in three rabbits, and the antibody was purified by affinity chromatography using antigen-conjugated resin (Sawady Technology, Inc., Tokyo, Japan). Rabbit polyclonal antibody anti-SOD1 was purchased from Assay Designs, Inc. (Ann Arbor, MI, USA). The secondary antibody (1 : 2500) was incubated with the membrane in TBS-T containing 2% skim milk, and washed six times with TBS-T. This rabbit and mouse secondary antibody was purchased from GE Healthcare Bio-Sciences (Tokyo). The blots were detected with an Immobilon Western Chemiluminescent HRP substrate (Millipore Corporation, Billerica, MA) and analyzed with a Lumino-image analyzer LAS-1000 plus (Fujifilm, Tokyo) according to the manufacturer's instructions.

Assay for SOD1 activity

Cells were suspended in 25 mM Tris-HCl buffer containing 1% Triton X-100, 50 mM bathocuproinedisulfonic acid, 1 mM EDTA, and a cocktail of protease inhibitors at pH 6.8, and then sonicated for 5 min. The supernatant was obtained by centrifugation of the lysate for 20 min at 16000 *g* at 4 °C. The protein samples were electrophoresed through 12.5%

non-denaturing polyacrylamide gel. Then, the gel was stained with nitroblue tetrazolium (NBT) to detect SOD activity.[18] SOD activity was detected as a decolorized band on the gel. The band was scanned and its digital image was quantified by NIH Image J 1.42 software. The assay was performed in three independent samples in each experimental group.

Real-time PCR

Total cellular RNA was extracted from MT-WT and MT-KO cells using Isogen (Nippon Gene, Tokyo). cDNA was synthesized from 0.2 μg of total RNA with a QuantiTect Reverse Transcription Kit (Qiagen, Tokyo). Amplification reactions were performed with SYBR® Premix Ex Taq™ II (Takara, Shiga, Japan). Gene-specific primers used for amplification of mouse CCS, Ctr1 (NM_175090), Atox1 (NM_009720), Cox17 (NM_017429), SOD1 (NM_011434), MT-I (NM_013602), MT-II (NM_008630), Atp7a, Atp7b and β-actin (NM_007393) cDNAs were as follows: CCS-forward (forward, F), 5′–CGGCCTAG-GCAGTGACAACA–3′; CCS-reverse (reverse, R), 5′–AGTC-GTCTGCACCAACACCATC–3′; Ctr1-(F), 5′–GACCACC-TCAGCCTCACACT–3′; Ctr1-(R), 5′–GGCATGGAATTG-TAGCGAAT–3′; Atox1-(F), 5′–TCAACAAGCTGGGAG-GAGTG–3′; Atox1-(R), 5′–ACATGGAAGCTTGCAGGG-AG–3′; Cox17-(F), 5′–TAGTCGGAGTTTGGGAGCTT–3′; Cox17-(R), 5′–ATTCACAAAGTAGGCCACCAC–3′; SOD1-(F), 5′–AGCATTCCATCATTGGCCGTA–3′; SOD1-(R), 5′–TT-TCCACCTTTGCCCAAGTCA–3′; MT-I-(F), 5′–CCTCTA-AGCGTCACCACGACTTC–3′; MT-I-(R), 5′–GGAGGTG-CACTTGCAGTTCTTG–3′; MT-II-(F), 5′–GCCTGCAAA-TGCAAACAATG–3′; MT-II-(R), 5′–GCACAGCAGCTG-CACTTGTC–3′; Atp7a-(F), 5′–TGGTAACCGGGAATGG-ATGATTAG–3′; Atp7a-(R), 5′–AACTCGGCCTCAGGT-TTCACAG–3′; Atp7b-(F), 5′–CAGCCAGAGCCATTGCT-ACTCA–3′; Atp7b-(R), 5′–GAAGGCAGTACCTCCGCA-AAGA–3′; β-actin-(F), 5′–CATCCGTAAAGACCTCTATG-CCAAC–3′; β-actin-(R), 5′–ATGGAGCCACCGATCCA-CA–3′. Samples were analyzed in triplicate in a total volume of 50 μL using an ABI PRISM 7000 Sequence Detection System (Applied Biosystems, Foster City, CA). β-Actin was used as the internal control for RNA quantification. RT-PCR was conducted under the following conditions: reverse transcription reaction of cDNA at 42 °C for 15 min, denaturation with reverse transcriptase at 95 °C for 3 min, followed by 40 cycles of PCR, *i.e.*, denaturation of cDNA at 95 °C for 15 s and annealing and extension at 60 °C for 1 min.

Determination and speciation of Cu in cells

MT-WT and MT-KO cells were seeded and treated with CCS-specific or control siRNA according to the same protocol as that mentioned above. After the treatment, the cells were collected, and the harvested cells were wet-ashed with nitric acid (analytical grade, Wako, Osaka, Japan) on a hot plate and then diluted with deionized water. Cu concentration in the samples was determined with an ICP-MS (Agilent7500ce, Agilent Technologies, Hachiouji, Japan) at m/z 65. The sample was pneumatically introduced into the ICP-MS through an interface consisting of a micro flow nebulizer (PFA-20, Glass Expansion, West Melbourne, Australia) coupled with a cyclone chamber (Glass Expansion). For the speciation of Cu and Zn, the cells were collected and suspended to a concentration of 2.0×10^4 cells μL^{-1} with 10 mM Tris–HCl, pH 7.2. The suspended cells were disrupted with an ultrasonic homogenizer (Bioruptors UCD-200, Cosmo Bio Ltd., Tokyo) on ice at 200 W, 20 kHz for 30 s three times at 30 s intervals. The cytosolic fraction was obtained by ultracentrifugation of the homogenate at 105 000 *g* for 60 min at 4 °C. The HPLC system (Prominence, Shimadzu, Kyoto, Japan) equipped with a narrow bore column was coupled with an ICP-MS (HPLC-ICP-MS) and used for metal speciation.[19] The narrow bore gel filtration column (Shodex Protein KW802.5-2E, 2.0 mm i.d. × 250 mm) was kindly provided by Showa Denko (Tokyo). A 5.0 μL aliquot of cytosol was applied to the column and the column was directly eluted with 100 mM ammonium acetate, pH 7.2, at a flow rate of 40 $\mu L\ min^{-1}$. The eluate was introduced into a micro concentric nebulizer (Ari Mist HP Nebulizer, Burgener, Ontario, Canada) connected to the cyclone chamber of the ICP-MS. The distributions of Cu and Zn in the eluate were monitored at m/z 65 and 66, respectively.

Evaluation of Atp7a and Atp7b functions in Cu efflux

MT-WT and MT-KO cells were seeded and treated with Atp7a- or Atp7b-specific or control siRNA according to the

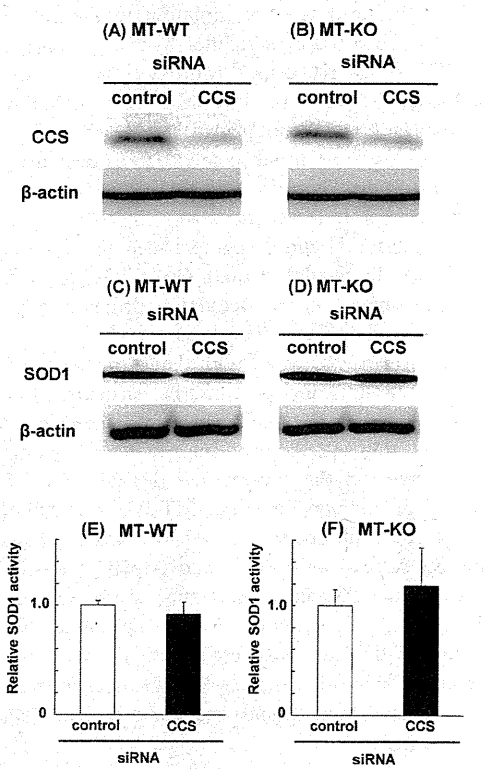

Fig. 1 Effects of CCS knockdown on CCS and SOD1 protein expression and SOD1 activity in MT-WT and MT-KO cells. CCS (A and B) and SOD1 (C and D) protein expression in MT-WT (A and C) and MT-KO (B and D) cells was determined by Western blotting. SOD1 activity in MT-WT (E) and MT-KO (F) cells was determined by nitroblue tetrazolium staining after native PAGE. SOD activity was detected as a decolorized band on the gel.

same protocol as that mentioned above. The cells transfected with siRNA were either exposed or not exposed to 10 μM copper acetate (Wako) plus 30 μM glutathione (GSH; Wako) for 24 h. Since Cu is transported into cells by Ctr1 as a monovalent ion, the complex of Cu(I) and GSH was used. After exposure to the Cu(I)-GSH complex, the cells were washed to remove Cu in the medium and continuously cultured in medium without Cu addition for another 24 h to evaluate the Cu efflux. Then, the cells were collected and wet-ashed with nitric acid to obtain the samples for Cu determination. Cu concentration was measured with an ICP-MS as mentioned above.

Statistics

Data are presented as means ± S.D. Statistical analysis involved one-way analysis of variance (ANOVA) followed by the Student's *t*-test. The levels of significant difference were set at $p < 0.05$ and 0.01 indicated by asterisks (*) and (**), respectively.

Results and discussion

Effects of CCS silencing on CCS and SOD1 expression and SOD1 activity

The protein expression levels of CCS in MT-WT and MT-KO cells decreased to 0.31 and 0.35, respectively, relative to the control when the cells were treated with CCS-targeting siRNA (Fig. 1A and B). There were no significant differences in cell viability between CCS and control siRNA transfected cells in both cell types (data not shown). Thus, this protocol was used to evaluate the effects of CCS knockdown in the following experiments.

As CCS plays a role in the delivery of Cu to SOD1, the expression and activity of SOD1 were evaluated in CCS-silenced MT-WT and MT-KO cells. There were no significant differences in the SOD1 expression between CCS and control siRNA transfected cells of both cell types (Fig. 1C and D). SOD1 activity was also not affected by the transfection of CCS-targeting siRNA in both MT-WT and MT-KO cells (Fig. 1E and F). Consequently, although CCS protein expression

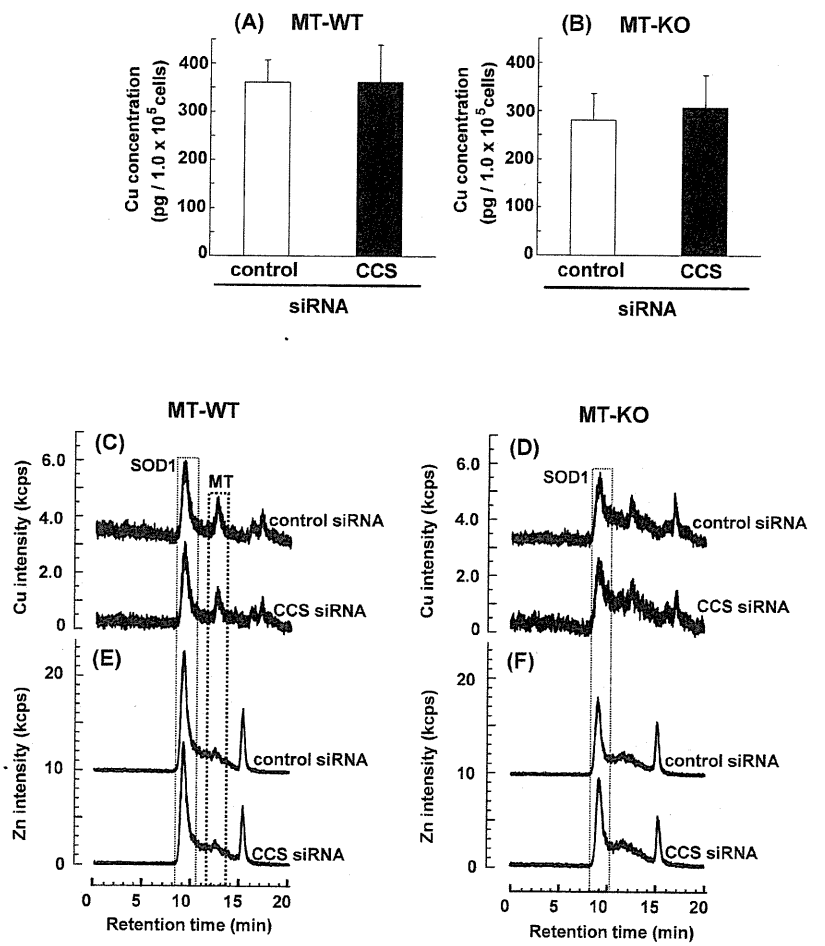

Fig. 2 Intracellular Cu concentration and distributions of Cu and Zn in MT-WT and MT-KO cells treated with CCS or control siRNA. Cu concentrations in MT-WT (A) and MT-KO (B) cells were determined with an ICP-MS equipped with a micro flow nebulizer at *m/z* 65. Data are expressed as means ± SD of three independent determinations. The distributions of Cu (C and D) and Zn (E and F) in MT-WT (C and E) and MT-KO (D and F) cells were determined with the narrow bore HPLC-ICP-MS. The column was eluted with 50 mM ammonium acetate, pH 7.0, at a flow rate of 40 μL min^{-1}. Cu and Zn in the eluate were monitored at *m/z* 65 and 66, respectively.

was actually suppressed by CCS-targeting siRNA, the protein expression and activity of SOD1 were not altered in MT-WT and MT-KO cells.

Cu concentration and distribution in CCS-silenced MT-WT and MT-KO cells

Cu concentrations in MT-WT and MT-KO cells were not changed by the transfection of CCS-targeting siRNA (Fig. 2A and B). Although there were no significant differences in the Cu concentration between MT-WT and MT-KO cells, MT-KO cells tended to have lower concentrations of Cu than MT-WT cells. This observation coincided with previous results.[12,15] To evaluate Cu distribution in the cytosolic fraction more precisely, the speciation of Cu by HPLC-ICP-MS was performed. Two major Cu peaks were detected in the chromatogram of MT-WT and MT-KO cells (Fig. 2C and D). The former peak contained not only Cu but also Zn, and its chromatographic behavior was identical to our previous report,[20] suggesting that it was assignable to SOD1. The amount of Cu bound to this peak was not changed by the CCS knockdown (Fig. 2C and D). The latter peak containing Cu was assignable to MT isoforms because its chromatographic behavior was identical to that previously reported.[20] In the elution profile of MT-KO cells, Cu was eluted at the retention time corresponding to MT (Fig. 2D). The peak containing Cu was also detected in the chromatogram of the liver supernatant of MT-KO mice (data not shown). An unidentified peak containing Cu remains in the chromatogram of the cytoplasmic fraction of MT-KO cells and perhaps also MT-WT cells. None of the peaks in the elution profiles could be assigned to CCS because the amount of CCS protein was estimated to be one-twelfth of that of SOD1 protein.[21] Thus, the estimated amount of CCS might be below the detection limit for Cu of the HPLC-ICP-MS under the current conditions.

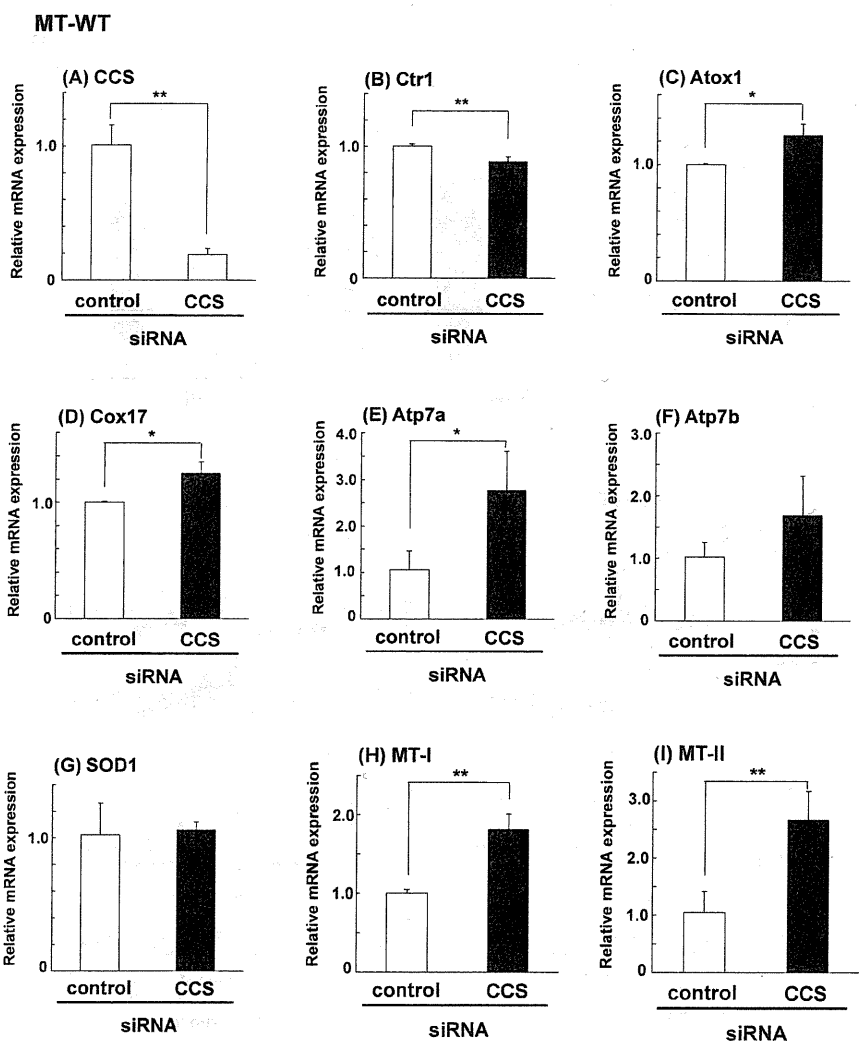

Fig. 3 mRNA expression of Cu-regulating genes in MT-WT cells treated with CCS-targeting or control siRNA. MT-WT cells were treated with CCS-targeting or control siRNA at 100 nM for 24 h. After the siRNA transfection, total RNA was isolated from the cells. The mRNA expression of Cu-regulating genes, such as CCS (A), Ctr1 (B), Atox1 (C), Cox17 (D), Atp7a (E), Atp7b (F), SOD1 (G), MT-I (H), and MT-II (I) was quantified by real-time PCR analysis and normalized to β-actin levels. Data are expressed as means ± S.D. of three independent determinations.

Consequently, the speciation study showed that Cu was constantly distributed in SOD1 in CCS-knockdown cells. No apparent changes in Zn distribution were noted between control and CCS-targeting siRNA treated cells (Fig. 2E and F).

Copper chaperones are required for the proper intracellular delivery of Cu to specific target proteins.[22] Indeed, it was shown that CCS is necessary and sufficient for the incorporation of Cu into SOD1 in the presence of a physiological level of Cu in eukaryotes.[23–25] It was also demonstrated that the marked reduction of SOD1 activity in tissues of CCS-KO mice ($CCS^{-/-}$) is caused by the impaired Cu incorporation into SOD1.[5] In the literature, SOD1 activity of $CCS^{-/-}$ was maintained at 10–20% in all tissues except the liver, and 30% in the liver of $CCS^{-/-}$ mice in spite of the lack of CCS. Protein blotting analysis showed that SOD1 protein levels in the tissues of $CCS^{-/-}$ were comparable to those of $CCS^{+/-}$ littermates. Hence, SOD1 protein properly received Cu from Cu proteins than CCS.

It was speculated that other Cu chaperones or MT compensated the role of CCS. In particular, Atox1 and CCS have a common motif, *i.e.*, MXCXXC, in the Cu-binding domain,[26,27] and the expression of other Cu chaperones was actually increased by the CCS knockdown. However, the handing over of Cu to SOD1 requires the formation of a heterodimer between SOD1 and CCS, and the heterodimer is formed on a specific domain of CCS, the so-called domain 3.[28] Thus, the formation of the heterodimers of SOD with other Cu chaperones seems to be not feasible. On the other hand, it was demonstrated that MT binding Cu (Cu-MT) was able to deliver Cu to apo-SOD1 in experiments that used both purified proteins.[14] However, as SOD1 activity was not affected by the CCS knockdown in MT-KO cells, MT could not play a crucial role in place of CCS in live cells.

Contrary to the animal experiments, no apparent decreases in the expression and activity of SOD1 were observed in CCS-knockdown cells (Fig. 1), and SOD1 protein expression was not completely abolished by CCS-targeting siRNA. This suggests that the remaining amount of CCS (31–35% of control) could be sufficient to deliver Cu to SOD1. In other

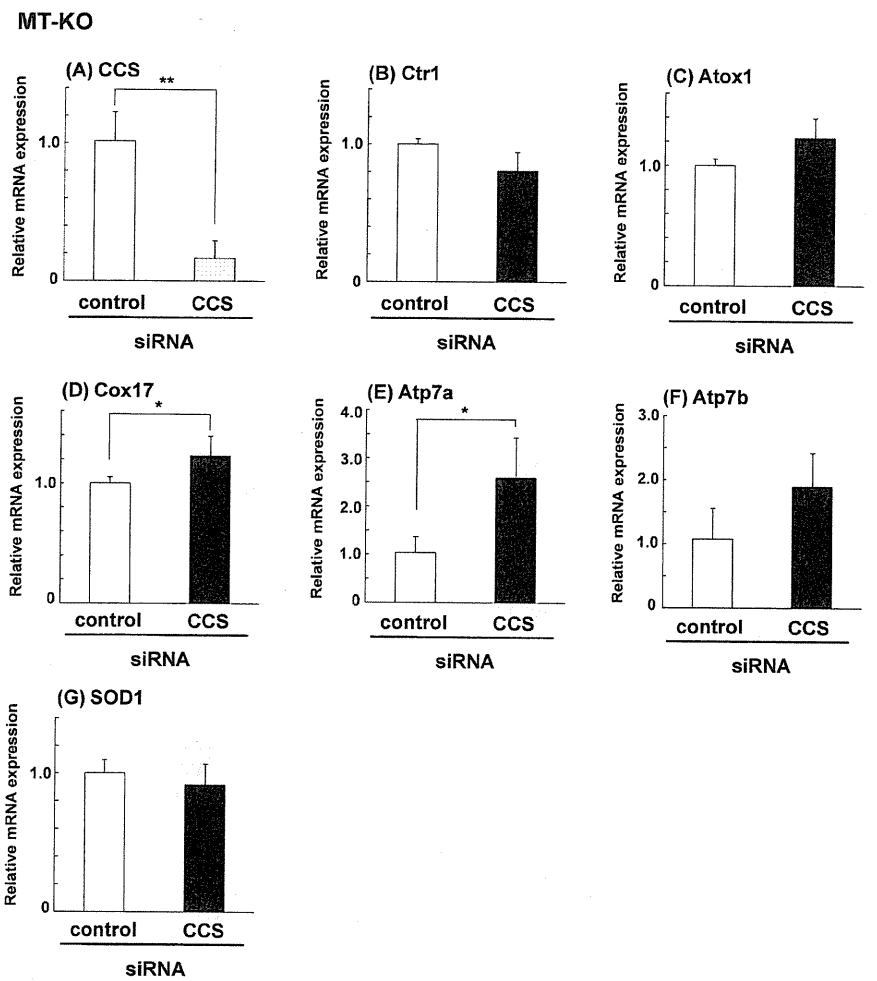

Fig. 4 mRNA expression of Cu-regulating genes in MT-KO cells treated with CCS-targeting or control siRNA. MT-KO cells were treated with CCS-targeting or control siRNA at 100 nM for 24 h. After the siRNA transfection, total RNA was isolated from the cells. The mRNA expression of Cu-regulating genes, such as CCS (A), Ctr1 (B), Atox1 (C), Cox17 (D), Atp7a (E), Atp7b (F), and SOD1 (G), was quantified by the real-time PCR analysis and normalized to β-actin levels. Data are expressed as means ± S.D. of three independent determinations.

words, the amount of CCS expressed may exceed that required for supplementation of Cu to SOD1 even under physiological conditions. The supplementation of Cu to SOD1 under the Cu-deficient condition was reported in blotchy mutant mice.[20] In the literature, blotchy mutant mice having a spontaneous mutation in the Atp7a gene showed systemic Cu deficiency and died within 3 weeks of age. Although the kidney of blotchy mice showed severe Cu deficiency, Cu supplementation to SOD1 was not affected. As another clinical feature, blotchy mice showed hypopigmentation due to a defect in tyrosinase activity, a cuproenzyme. This indicates that Cu supplementation to SOD1 may be predominant compared to other cuproenzymes, at least tyrosinase, and the predominant Cu supplementation to SOD1 may be due to the abundant expression of its specific chaperone, CCS. In addition, it can be suggested that redundant CCS acts as a Cu chaperone and plays other roles in the cells as well. Indeed, it was reported that CCS increased the expression of the reduced form of SOD1 due to its anti-oxidative property.[28]

Determination of mRNA expression of Cu-related genes in CCS-silenced MT-WT and MT-KO cells

The mRNA expression of CCS in MT-WT and MT-KO cells transfected with CCS-targeting siRNA decreased to 0.19 and 0.17, respectively, relative to cells transfected with control siRNA (Fig. 3A and 4A). CCS knockdown significantly decreased Ctr1 mRNA expression compared to the control in MT-WT cells (Fig. 3B), while Ctr1 mRNA expression in MT-KO cells showed a tendency to decrease with the transfection of CCS-targeting siRNA, similar to the case of MT-WT cells (Fig. 4B). On the other hand, CCS knockdown significantly increased the mRNA expression of Atox1 and Cox17 to 1.25 and 1.23 times higher than those of the control in MT-WT cells, respectively (Fig. 3C and D), and that in MT-KO cells showed the same tendency as well (Fig. 4C and D). Moreover, CCS knockdown significantly increased Atp7a mRNA expression to 3.00 and 2.50 times higher than those of control in MT-WT and MT-KO cells, respectively (Fig. 3E and 4E), and Atp7b mRNA expression showed the same tendency as Atp7a mRNA expression (Fig. 3F and 4F). Meanwhile, SOD1 mRNA expression was not affected by the transfection of CCS-targeting siRNA in both cell types (Fig. 3G and 4G). This was coincident with the protein expression and activity of SOD1 (Fig. 1C, D, E, and F). The mRNA expression of MT-I and MT-II in MT-WT cells was increased to 1.80 and 2.70, respectively, by the transfection of CCS-targeting siRNA (Fig. 3H and I). Such observations as the decrease in Ctr1 mRNA expression and the increase in Atp7a, Cox17, and MT expression could reflect the response to the excess Cu of CCS-knockdown MT-WT and MT-KO cells.

Ctr1 mRNA expression was decreased in CCS-silenced MT-WT and MT-KO cells. Ctr1 functions in the high-affinity uptake of Cu on the plasma membrane of various mammalian cells,[29–31] and thus, the decrease in Ctr1 mRNA expression is an indication that the cells responded to the excess Cu. On the other hand, the expression of Atp7a and 7b was increased by the CCS knockdown. These Cu-transporting ATPases can act as a Cu-efflux pump and thus, it is straightforward to assume that the increases in Atp7a and Atp7b expression are also a response to the excess Cu. However, Cu concentration in the cells and its distribution in the cytoplasmic fraction were not altered by CCS silencing. Namely, it could be explained that increased Atp7a and/or Atp7b contribute to maintain the intracellular Cu level in CCS-silenced cells. Hence, to evaluate the responsibilities of Atp7a and Atp7b, either ATPases were silenced, and the Cu concentration in MT-WT and MT-KO bearing Atp7a or Atp7b knockdown.

Contribution of Atp7a and Atp7b to the Cu efflux in MT-WT and MT-KO cells

The mRNA expression levels of Atp7a and Atp7b in MT-WT cells introduced with the specific siRNAs were significantly decreased to 0.20 and 0.23 of those of control siRNA-introduced cells, respectively (Fig. 5A and B). On the other hand, the mRNA expression levels of Atp7a and Atp7b in MT-KO cells were also significantly decreased to 0.28 and 0.24, respectively (Fig. 5C and D). These indicated that both Atp7a and Atp7b were expressed in MT-WT and MT-KO cells, and siRNAs used in this study were able to actually reduce the expressions of Atp7a and Atp7b in both cell lines.

The Cu concentration in MT-WT cells were significantly increased by the introduction of siRNA targeting Atp7a, suggesting that the Cu efflux in MT cells were inhibited by

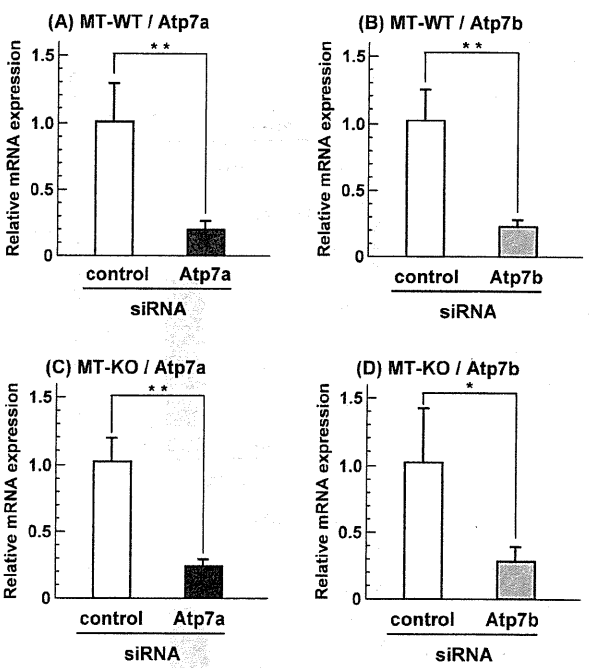

Fig. 5 mRNA expression of Cu-transporting ATPase genes in MT-WT and MT-KO cells treated with Atp7a- or Atp7b-targeting or control siRNA. MT-WT and MT-KO cells were treated with Atp7a- or Atp7b-targeting or control siRNA at 100 nM for 24 h. After the siRNA transfection, total RNA was isolated from the cells. The mRNA expression of Cu-transporting ATPase genes, such as Atp7a (A and C) and Atp7b (B and D) in MT-WT (A and B) and MT-KO (C and D), was quantified by the real-time PCR analysis and normalized to β-actin levels. Data are expressed as means ± S.D. of three independent determinations.

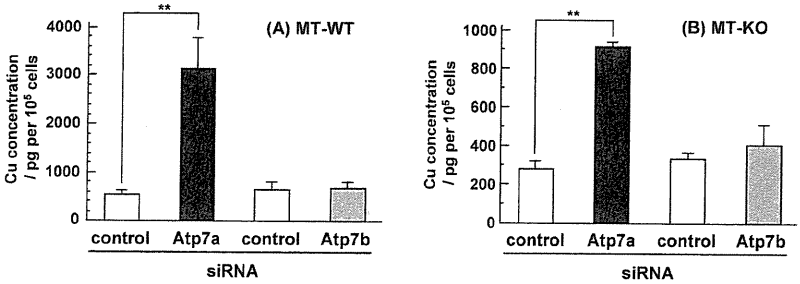

Fig. 6 Intracellular Cu concentration in MT-WT and MT-KO cells treated with Atp7a- or Atp7b-targeting or control siRNA. MT-WT and MT-KO cells treated with Atp7a- or Atp7b-targeting or control siRNA were exposed 10 μM Cu(I)-GSH complex for 24 h. Then, the Cu(I)-GSH complex was removed from the medium and the cells were cultured for additional 24 h. Cu concentrations in MT-WT (A) and MT-KO (B) cells were determined with an ICP-MS equipped with a micro flow nebulizer at *m/z* 65. Data are expressed as means ± SD of three independent determinations.

silencing Atp7a (Fig. 6A, closed column). There were no significant effects of Apt7b silencing on the Cu concentration in MT-WT cells (Fig. 6A, hatched column). Although MT-KO cells accumulated less Cu than MT-WT as reported previously,[15] the results obtained by silencing either ATPase in MT-KO showed the same tendency as those in MT-WT (Fig. 6B). Namely, that the Atp7a knockdown induced Cu accumulation despite Atp7b knockdown not having a significant affect. These results suggest that Atp7a mainly contributes to the Cu efflux in these cell lines, fibroblasts, being independent of the existence of MT. Indeed, this observation was coincident with the gene responses caused by the CCS knockdown (Fig. 3 and 4). The CCS knockdown significantly and specifically induced the Atp7a expression but not Atp7b (Fig. 3E, F, 4E and F) in addition to the reduction of Ctr1 expression. Atp7a substantially responded to the Cu efflux rather than Atp7b (Fig. 6), thus, the maintenance of the intracellular Cu levels in the cells (Fig. 2) would be attributed to these gene responses.

Conclusions

SOD1 activity was maintained in cells even when the amount of CCS was reduced to 0.31–0.35 of the control level by the specific targeting of siRNA. This suggests that the amount of CCS expressed may exceed that required to supply Cu to SOD1. The CCS knockdown caused Cu repletion in the cells, and the Cu-regulating genes, *i.e.*, Ctr1 and Atp7a responded to the Cu repletion resulting in the maintenance of the intracellular Cu level. Our results demonstrate a novel and quantitative relationship between CCS and SOD1, and quantitative contribution of Atp7a and Atp7b in Cu homeostasis.

Acknowledgements

The authors would also like to acknowledge Grants-in-Aid from the Ministry of Education, Culture, Sports, Science and Technology, Japan (Nos. 09J04232 for TM and 19390033 for YO), and the financial support from Agilent Technologies Foundation, USA. The authors wish to thank Showa Denko for providing the narrow bore column and the HPLC system.

References

1 E. J. Massaro, in *Handbook of Copper Pharmacology and Toxicology*, Humana Press, Totowa, 2003.
2 B. E. Kim, T. Nevitt and D. J. Thiele, *Nat. Chem. Biol.*, 2008, **4**, 176–185.
3 J. Lee, J. R. Prohaska, S. L. Dagenais, T. W. Glover and D. J. Thiele, *Gene*, 2000, **254**, 87–96.
4 B. Zhou and J. Giyschier, *Proc. Natl. Acad. Sci. U. S. A.*, 1997, **94**, 7481–7486.
5 P. C. Wong, D. Waggoner, J. R. Subramaniam, L. Tessarollo, T. B. Bartnikas, V. C. Culotta, D. L. Price, J. Rothstein and J. D. Gitlin, *Proc. Natl. Acad. Sci. U. S. A.*, 2000, **97**, 2886–2891.
6 L. W. Klomp, S. J. Lin, D. S. Yuan, R. D. Klausner, V. C. Culotta and J. D. Gitlin, *J. Biol. Chem.*, 1997, **272**, 9221–9226.
7 I. Hamza, M. Schaefer, L. W. Klomp and J. D. Gitlin, *Proc. Natl. Acad. Sci. U. S. A.*, 1999, **96**, 13363–13368.
8 Y. C. Horng, S. C. Leary, P. A. Cobine, F. B. J. Young, G. N. George, E. A. Shoubridge and D. R. Winge, *J. Biol. Chem.*, 2005, **280**, 34113–34122.
9 Y. C. Horng, P. A. Cobine, A. B. Maxfield, H. S. Carr and D. R. Winge, *J. Biol. Chem.*, 2004, **279**, 35334–35340.
10 A. Presta and M. J. Stillman, *J. Inorg. Biochem.*, 1997, **66**, 231–240.
11 M. T. Salgado and M. J. Stillman, *Biochem. Biophys. Res. Commun.*, 2004, **318**, 73–80.
12 Y. Ogra, M. Aoyama and K. T. Suzuki, *Arch. Biochem. Biophys.*, 2006, **451**, 112–118.
13 K. T. Suzuki, A. Someya, Y. Komada and Y. Ogra, *J. Inorg. Biochem.*, 2002, **88**, 173–182.
14 K. T. Suzuki and T. Kuroda, *Res. Commun. Mol. Pathol. Pharmacol.*, 1995, **87**, 287–296.
15 T. Miyayama, K. T. Suzuki and Y. Ogra, *Toxicol. Appl. Pharmacol.*, 2009, **237**, 205–213.
16 Y. Kondo, T. Yanagiya, S. Himeno, Y. Yamabe, D. Schwartz, M. Akimoto, J. S. Lazo and N. Imura, *Life Sci.*, 1999, **64**, 145–150.
17 A. S. Payne, E. J. Kelly and J. D. Gitlin, *Proc. Natl. Acad. Sci. U. S. A.*, 1998, **95**, 10854–10859.
18 C. Beauchamp and I. Fridovich, *Anal. Biochem.*, 1971, **44**, 276–287.
19 T. Miyayama, D. Hiraoka, F. Kawaji, E. Nakamura, N. Suzuki and Y. Ogra, *Biochem. J.*, 2010, **429**, 53–61.
20 T. Miyayama, Y. Ogra, Y. Osima and K. T. Suzuki, *Anal. Bioanal. Chem.*, 2008, **390**, 1799–1803.
21 E. C. West and J. R. Prohaska, *Exp. Biol. Med.*, 2004, **229**, 756–764.
22 V. C. Culotta, S. J. Lin, P. Schmidt, L. W. Klomp, R. L. Casareno and J. Gitlin, *Adv. Exp. Med. Biol.*, 1999, **448**, 247–254.
23 V. C. Culotta, L. W. Klomp, J. Strain, R. L. Casareno, B. Krems and J. D. Gitlin, *J. Biol. Chem.*, 1997, **272**, 23469–234672.
24 T. D. Rae, P. J. Schmidt, R. A. Pufahl, V. C. Culotta and T. V. O'Halloran, *Science*, 1999, **284**, 805–808.

25 L. B. Corson, V. C. Culotta and D. W. Cleveland, *Proc. Natl. Acad. Sci. U. S. A.*, 1998, **95**, 6361–6366.
26 R. A. Pufahl, C. P. Singer, K. L. Peariso, S. J. Lin, P. J. Schmidt, C. J. Fahrni, V. C. Culotta, J. E. Penner-Hahn and T. V. O'Halloran, *Science*, 1997, **278**, 853–856.
27 P. J. Schmidt, T. D. Rae, R. A. Pufahl, T. Hamma, J. Strain and T. V. O'Halloran, *J. Biol. Chem.*, 1999, **274**, 23719–23725.
28 J. B. Proescher, M. Son, J. L. Elliott and V. C. Culotta, *Hum. Mol. Genet.*, 2008, **17**, 1728–1737.
29 J. Lee, M. M. Peña, Y. Nose and D. J. Thiele, *J. Biol. Chem.*, 2002, **277**, 4380–4387.
30 S. Puig and D. J. Thiele, *Curr. Opin. Chem. Biol.*, 2002, **6**, 171–180.
31 J. F. Eisses, Y. Chi and J. H. Kaplan, *J. Biol. Chem.*, 2005, **280**, 9635–9639.

Anal Bioanal Chem (2011) 399:1765–1772
DOI 10.1007/s00216-010-4143-4

ORIGINAL PAPER

Distribution and metabolism of selenohomolanthionine labeled with a stable isotope

Yasumi Anan · Takahiro Mikami · Yoshiro Tsuji · Yasumitsu Ogra

Received: 30 June 2010 / Revised: 16 August 2010 / Accepted: 18 August 2010 / Published online: 6 September 2010

Abstract The distribution and metabolism of selenohomolanthionine (4,4′-selenobis[2-aminobutanoic acid], SeHLan), a newly identified selenoamino acid in selenized Japanese pungent radish, were evaluated by administering ^{77}Se-labeled SeHLan at a dose of 25 μg/kg body weight in rats. Exogenous ^{77}Se of SeHLan was preferably distributed to the kidneys and remained in the intact form for up to 6 h after dosing. The accumulation in the kidneys is one of the specific characteristics of SeHLan, differing from other selenoamino acids, such as selenomethionine and *Se*-methylselenocysteine, which preferably accumulate in the pancreas. The intact form of SeHLan was detected in the serum and kidney supernatant but not in the urine, suggesting that the amount of exogenous Se that was distributed to the kidneys was within metabolic capacity. Indeed, the exogenous Se was converted into two urinary metabolites, *Se*-methylseleno-*N*-acetyl-galactosamine and trimethylselenonium. Exogenous Se was also detected in several selenoproteins, including selenoprotein P and extracellular glutathione peroxidase. SeHLan is expected to be a potential supplemental source of Se because its distribution differs from that of selenomethionine and *Se*-methylselenocysteine.

Keywords Selenohomolanthionine · Stable isotope · Selenium · Speciation · ICP-MS

Published in the special issue *Speciation Analysis in Healthcare* with Guest Editor Heidi Goenaga Infante.

Y. Anan · Y. Ogra
Laboratory of Chemical Toxicology and Environmental Health, Showa Pharmaceutical University, Machida, Tokyo 194-8543, Japan

Y. Anan · T. Mikami · Y. Tsuji
Graduate School of Pharmaceutical Sciences, Chiba University, Chiba 260-8675, Japan

Y. Ogra (✉)
High Technology Research Center, Showa Pharmaceutical University, Machida, Tokyo 194-8543, Japan
e-mail: ogra@ac.shoyaku.ac.jp

Introduction

Selenium (Se) exists in nature in various chemical forms, such as inorganic salts, selenoamino acid derivatives, and selenosugars [1]. These selenocompounds can be utilized as a nutritional source despite variations in their assimilation efficacies [2]. Among the selenocompounds, selenoamino acid derivatives are usually used as a supplemental source because they are less toxic than inorganic Se salts and their assimilation efficacy is superior to that of selenosugars [3]. Se-fortified (selenized) yeast and vegetables have been developed for use as a supplemental source of Se because they can be efficiently metabolized to yield selenoamino acid derivatives from inorganic Se, thereby resulting in the high accumulation of Se in the form of selenoamino acid derivatives. Selenized yeast is the most popular Se source because of its rapid growth, ease of culture, and high Se accumulation capacity. It was reported that selenized yeast contained selenomethionine (SeMet), such as SeMet derivatives as *Se*-adenosylselenomethionine, SeMet-containing proteins, and other selenoamino acids [4, 5]. *Brassicaceae* and *Alliaceae* plants, such as Indian mustard (*Brassica juncea*) and garlic (*Allium sativum*), are also known as Se accumulators. These plants are fortified with Se and accumulate Se in the form of *Se*-methylselenocysteine (MeSeCys), γ-glutamyl-*Se*-methylselenocysteine (GulMeSeCys) [6, 7]. MeSeCys and its derivative are expected to